ACS Catalysis

Research Article

pubs.acs.org/acscatalysis

Ruthenium Olefin Metathesis Catalysts Containing Fluoride

Stefano Guidone,[†] Olivier Songis,[†] Laura Falivene,[‡] Fady Nahra,[†] Alexandra M. Z. Slawin,[†] Heiko Jacobsen,[§] Luigi Cavallo,[‡] and Catherine S. J. Cazin*[,†]

[†]EaStCHEM School of Chemistry, University of St Andrews, St. Andrews KY16 9ST, United Kingdom

[‡]Physical Sciences and Engineering, Catalysis Center, King Abdullah University of Science and Technology (KAUST), Thuwal 23955-6900, Saudi Arabia

[§]KemKom, 1215 Ursulines Avenue, New Orleans, Louisiana 70116, United States

Supporting Information

ABSTRACT: The reaction of the ruthenium complex *cis*-**Caz-1** with silver fluoride affords the first example of an active olefin metathesis precatalyst containing fluoride ligands. The cis geometry of the precursor complex is key to the successful fluoride exchange reaction. Computational studies highlight the stability of the new Ru−F species, due to push−pull interactions between fluoride and L-type ligands (L: *N*-heterocyclic carbene, phosphite). Insights into the isomerization process from *trans*-**Caz-1** to *cis*-**Caz-1** are given. Fluoride exchange reactions were performed involving *cis*- and *trans*-**Caz-1** complexes. Catalytic tests showcase the excellent activity of the Ru−F containing complexes.

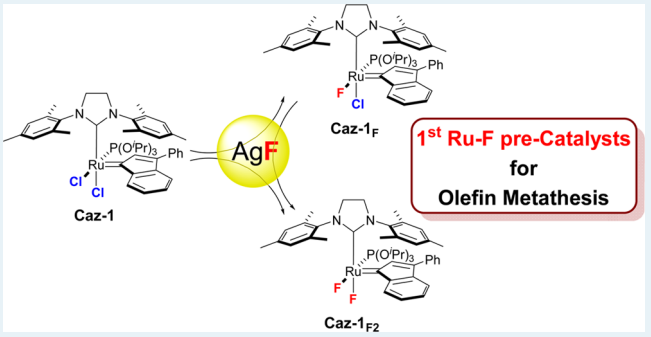

KEYWORDS: *olefin metathesis, homogeneous catalysis, ruthenium, fluoride, halide exchange*

INTRODUCTION

The introduction of fluorine atoms in molecules can drastically change their physical and chemical properties.[1] Organofluorine compounds are nowadays employed in the agrochemical and pharmaceutical industry, with an ever increasing demand for this class of compounds.[2] Fluorine has been introduced into metal complexes as a fluoride ligand.[3] Late-transition-metal fluoride complexes represent a challenge in synthetic organometallic chemistry because of the hard−soft mismatch.[2,4] As a result, only a limited number of examples of transition metal fluoride complexes (namely, Pd,[5a] Pt,[5b] Ir,[5c] Os,[5d−f] and Ru[5e−k]) have been disclosed to date. Most synthetic protocols leading to M−F bond formation involve an oxidative addition of XeF_2 in anhydrous HF or reaction with $Et_3N{\cdot}3HF$.[4d,f,5d,6] Oxidative addition of organofluoro compounds via C−F bond activation can be performed, but it is somewhat limited to group 9−10 metals.[7] An alternative strategy to access M−F compounds consists of halide-exchange reactions that can be carried out under relatively mild reaction conditions using reagents such as CsF,[4c,d] AgF,[4f] NMe_4F,[3h,4g] and $[(Me_2N)_3S]^+[Me_3SiF_2]^-$ (TASF).[4h] Such synthetic methods have been applied to ruthenium, leading to fluoride complexes, as shown in Figure 1. Caulton and co-workers have reported the synthesis of $[Ru(F)(H)(CO)(P^tBu_2Me)_2]$ through halide exchange reactions using CsF.[4c] More recently, Whittlesey and co-workers have shown that complexes of type $[Ru(F)(H)(CO)L_n]$ (n = 2,3; L = PR_3, NHC) could be isolated using $Et_3N{\cdot}3HF$ as the fluorinating agent.[8] In all complexes reported by Caulton and Whittlesey, a square pyramidal or an octahedral geometry is adopted with the fluoride ligand trans to the π-acceptor CO (Figure 1). A push−pull interaction between the fluoride (here

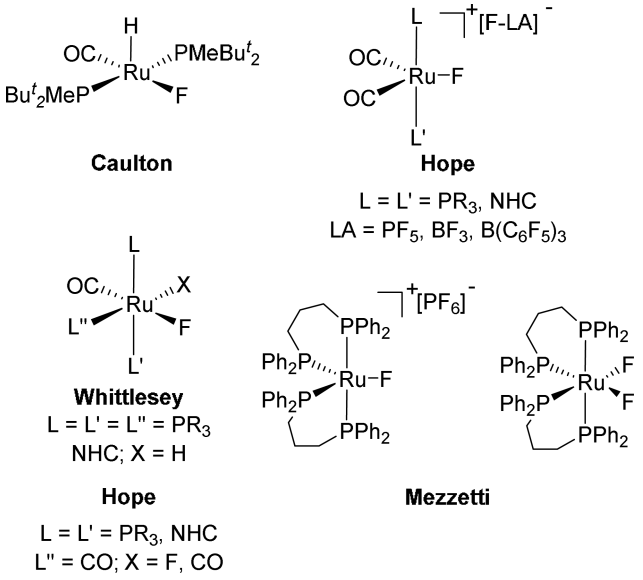

Figure 1. Ruthenium fluoride complexes.

Received: February 3, 2015
Revised: May 13, 2015

DOI: 10.1021/acscatal.5b00219
ACS Catal. 2015, 5, 3932−3939

acting as a π-donor) and the trans carbonyl ligand is invoked to stabilize the Ru−F bond.

Difluoride Ru clusters such as $[RuF_2(CO)_3]_4$[5i−k] developed by Wilson and co-workers and derivatives obtained by substitution of carbonyls with phosphines[5f] and *N*-heterocyclic carbenes (NHC)[5h] were reported by Hope and co-workers. The reactivity of the 18e$^-$-difluoride complexes $[RuF_2(CO)_2L_2]$ (L = PR_3, NHC) toward Lewis acids (LA) (e.g., PF_5, BF_3, and $B(C_6F_5)_3$) has led to the corresponding 16e$^-$-cationic species, in which the counterion has a stabilizing effect on the complex.[5g,h] All reports on Ru-carbonyl complexes contrast with the cationic monofluoride and the neutral difluoride species developed by Mezzetti and co-workers (Figure 1).[3g,h] This last cationic complex was obtained through halide exchange of $[RuCl(dppp)_2]PF_6$ with TlF (dppp = 1,3-bis(diphenylphosphino)propane), and further reacted with NMe_4F to yield the neutral difluoride species. In these complexes, the fluoride ligand is described as a poor π-donor ligand, resulting in a simple electrostatic interaction between a cationic ruthenium species and fluoride. To the best of our knowledge, no other type of Ru complex bearing a F ligand has been reported to date. Complexes that would be of great interest would be Ru−F-containing congeners of alkene metathesis active systems. Indeed, kinetic studies by Grubbs and co-workers showed that the catalytic activity of complexes of the type $[RuX_2(SIMes)(=CHPh)]$ (X = Cl, Br, I, SIMes = *N*,*N*′-bis[2,4,6-(trimethyl)phenyl]imidazolidin-2-ylidene) decreases in the order Cl > Br > I, suggesting a possibly higher efficiency for the fluoride analogues.[9] Computational studies on the formation of ruthena(IV)cyclobutanes from first- and second-generation Grubbs precatalysts and norborn-2-ene have illustrated a similar trend of reactivity for dihalide complexes (F > Cl > Br > I), predicting the best activity of difluoride species among olefin metathesis precatalysts.[10] Despite this insight into possible reactivity, whereas bromide/iodide/carboxylate versions of Grubbs and Hoveyda−Grubbs type complexes have been extensively studied,[9,11] no fluoride version has, to the best of our knowledge, been reported to date. A few failed attempts using HF or AgF suggest that these methodologies or Grubbs/Hoveyda−Grubbs type complexes are not suitable for the synthesis of Ru−F species for olefin metathesis.[12] Recently, we have developed a new class of Ru-olefin metathesis catalysts that display an unusual cis geometry and lead to outstanding stability and activity in olefin metathesis reactions.[13] It appeared therefore of great interest to evaluate the ability of such complexes to undergo chloride exchange with fluoride. Herein, we report our findings on chloride exchange reactions using a number of olefin metathesis precatalysts.

RESULTS AND DISCUSSION

Chloride Exchange with AgF. The reactivity of various commercially available precatalysts with AgF as a fluoride source was initially examined (Figure 2).

The reaction of **Ind-II**, **Ind-III**, and **Hov-II** with AgF showed no conversion of the starting material after 1 h (Table 1, entries 1−3). In contrast, under the same reaction conditions, the phosphite-containing complex *trans*-**Caz-1** leads to 10% conversion of the starting material into the monofluorinated species (Table 1, entry 4). With longer reaction time (24 h), 53% of *trans*-**Caz-1** was converted into a Ru−F species (Table 1, entry 5). Monitoring this reaction for a few hours showed a reaction rate similar to the one involved in the trans−cis isomerization of the complex.[14] We therefore reasoned that isomerization might be required before chloride exchange. If such were the case, the cis complex should show a superior reactivity. *Cis*-**Caz-1** was thus reacted with AgF. A very rapid reaction occurred with a 76% conversion leading to the same fluorinated product obtained from *trans*-**Caz-1** (Table 1, entry 6). Using 2 equiv of AgF, full conversion of the starting material was observed with both mono- and difluoride products formed. Using only 20% excess of AgF leads to the selective formation of the monofluorinated product (Table 1, entries 7 and 8). Increasing the amount of AgF to 2.4 equiv leads to the quantitative formation of the difluoride species (Table 1, entry 9).

Table 1. Chloride Exchange with AgF[a]

entry	precatalyst	AgF equiv	[Ru]Cl_2 species[b]	[Ru]ClF species[b]	[Ru]F_2 species[b]
1	**Ind-II**	1	100	n.r.	n.r.
2	**Ind-III**	1	100	n.r.	n.r.
3	**Hov-II**	1	100	n.r.	n.r.
4	*trans*-**Caz-1**	1	90	10	
5	*trans*-**Caz-1**	1	47[c]	53[c]	
6	*cis*-**Caz-1**	1	24	76	
7	*cis*-**Caz-1**	1.2		>99	
8	*cis*-**Caz-1**	2		21	79
9	*cis*-**Caz-1**	2.4			>99

[a]Reaction conditions: complex (0.01 mmol), AgF (1−2.4 equiv), CD_2Cl_2 (0.6 mL), rt, 1 h. [b]Conversion (%) determined by ^{1}H NMR. [c]24 h.

Synthesis of [Ru(Cl)(F)(Ind)(SIMes){P(O^{i}Pr)$_3$}], Caz-1$_F$. **Caz-1$_F$** was quantitatively obtained by reaction of 1 equiv of *cis*-**Caz-1** with 1.2 equiv of AgF. The ^{1}H NMR spectrum contains a characteristic doublet at 8.93 ppm assigned to the indenylidene (Ind) H^7 proton, which is shifted downfield compared with the signal observed for *cis*-**Caz-1**. In the ^{31}P−{^{1}H} NMR spectrum, a doublet is observed at 131.4 ppm ($^2J_{PF}$ = 286 Hz) corresponding to the phosphite ligand. This signal is also shifted downfield compared with the ^{31}P signal of the starting material.[13a] In the ^{19}F−{^{1}H} NMR spectrum, a doublet at −217.2 ppm ($^2J_{PF}$ = 286 Hz) is found. These data are consistent with a trans disposition of the fluorine and phosphite ligands. The ^{13}C−{^{1}H} NMR spectrum contains a doublet at 289.6 ppm ($^2J_{CP}$ = 25.5 Hz) and a doublet at 209.1 ppm ($^2J_{CP}$ = 16.0 Hz) corresponding to the carbene carbon atom of the indenylidene and of the *N*-heterocyclic carbene, respectively. The structure was unambiguously confirmed by single-crystal X-ray diffraction (Figure 3).[15]

Caz-1$_F$ presents a slightly distorted square pyramidal geometry with the indenylidene unit sitting at the apical position. Hydrogen bonding (dashed line) between H^7 of the indenylidene ring and the fluorine atom is observed, which might explain the smaller C_{Ind}−Ru−F angle (102.82(13)°) observed compared with the dichloride analogue (104.3(2)°).[13a] Similar intramolecular F···H interactions have also been observed by Hope and co-workers.[5f]

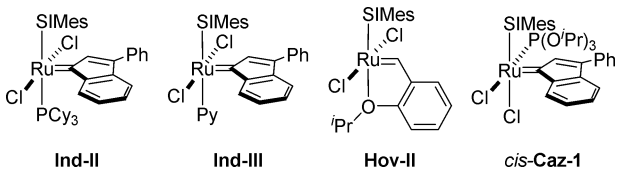

Figure 2. Olefin metathesis precatalysts tested in Cl exchange.

DOI: 10.1021/acscatal.5b00219
ACS Catal. 2015, 5, 3932−3939

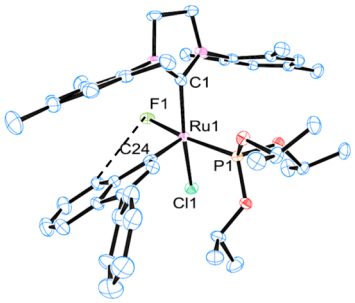

Figure 3. Molecular structure of **Caz-1$_F$**. All solvent molecules and hydrogen atoms are omitted for clarity. Thermal ellipsoids are shown at the 50% probability level.

Synthesis of [RuF$_2$(Ind)(SIMes){P(O^{i}Pr)$_3$}], Caz-1$_{F2}$. The difluorinated complex **Caz-1$_{F2}$** was quantitatively obtained by reaction of *cis*-**Caz-1** with 2.4 equiv of AgF. The ^{1}H NMR spectrum contains a characteristic doublet at 9.02 ppm corresponding to the indenylidene H^7 proton, which is shifted downfield compared with **Caz-1$_F$** (8.93 ppm) and *cis*-**Caz-1** (8.87 ppm).[13a] In the ^{31}P−{^{1}H} NMR spectrum, a doublet at 131.5 ppm ($^2J_{PF}$ of 286 Hz) corresponding to the phosphite ligand is observed. This signal is also shifted downfield compared with the ^{31}P signals of **Caz-1$_F$** and *cis*-**Caz-1**.[13a] The ^{19}F-{^{1}H} NMR spectrum contains a doublet at −217.7 ppm ($^2J_{PF}$ = 286 Hz) corresponding to the fluoride trans to the phosphite, and a broad singlet at −237.2 ppm corresponding to the second fluoride, which is cis to the phosphite ligand. The ^{13}C−{^{1}H} NMR was recorded at 223 K. The spectrum contains two broad signals at 287.0 and 211.1 ppm corresponding to the carbene carbon atom of the indenylidene and of the *N*-heterocyclic carbene, respectively. The structure of the complex was confirmed by X-ray diffraction on s single crystal (Figure 4).[16]

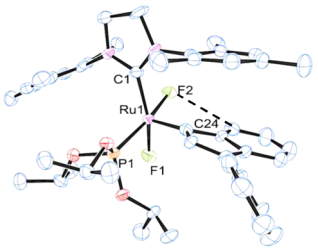

Figure 4. Molecular structure of **Caz-1$_{F2}$**. All solvent molecules and hydrogen atoms are omitted for clarity. Thermal ellipsoids are shown at the 50% probability level.

A similar interaction (dashed line) between H^7 of indenylidene ring and the fluorine atom trans to the phosphite is observed, presumably responsible for the relatively small C$_{Ind}$−Ru−F angle (103.39(17)°) compared with the dichloride analogue (104.3(2)°).[13a] Both complexes display a distorted square pyramidal geometry with the phosphite ligand cis to the NHC (P−Ru−C$_{NHC}$ angles being 97.66(10)° and 97.82(14)° for **Caz-1$_F$** and **Caz-1$_{F2}$**, respectively) (Table 2).

In both complexes, the Ru−F bond is significantly shorter than the Ru−Cl. For all complexes, comparable Ru−C (NHC and indenylidene) bond lengths are found, whereas Ru−P bond distances show some disparity. The latter decreases in the following order: *cis*-**Caz-1** > **Caz-1$_F$** > **Caz-1$_{F2}$**, which reflects the electronegativity of F vs Cl.

Table 2. Selected Bond Distances (Å), Angles (deg)(esd)

Ru(1)−X$_{transP}$	2.4036(18)	2.029(3)	2.017(3)
Ru(1)−X$_{transNHC}$	2.3974(19)	2.3837(12)	2.035(4)
Ru(1)−P(1)	2.249(2)	2.2426(11)	2.2263(16)
Ru(1)−C(24)	2.067(7)	2.059(4)	2.053(6)
Ru(1)−C(1)	1.881(8)	1.864(5)	1.846(6)
P(1)−Ru(1)−C(24)	100.6(19)	97.66(10)	97.82(14)
P(1)−Ru(1)−C(1)	90.5(2)	90.19(12)	89.95(15)
C(24)−Ru(1)−C(1)	98.7(3)	97.09(17)	96.1(3)

Chloride Exchange and Isomerization Studies. Braddock and co-workers have reported a study using Hoveyda−Grubbs precatalysts of the type [RuX$_2$(SIMes)(=CH−2-(^{i}PrO)−C$_6$H$_4$)] where X is Cl, Br, CF$_3$CO$_2$, and C$_2$F$_5$CO$_2$.[11d] When reacting two complexes containing different pairs of anionic ligands (1:1 molar ratio), a statistical mixture of 1:2:1 was obtained, in which a novel complex with mixed anions is in equilibrium with the starting materials (pseudodegenerate ligand exchange).[11d] This encouraged us to investigate the ability of our dichloro and difluoro species to be involved in such an exchange (Table 3).

Table 3. Fluoride Exchange Reactions

entry	complex	time (h)	conversion to **Caz-1$_F$** (%)[a]
1	**Caz-1$_{F2}$** + *cis*-**Caz-1**	0.5	>99
2	**Caz-1$_{F2}$** + *trans*-**Caz-1**	0.5	30
3		1.5	40
4		24	>99

[a]Determined by ^{1}H NMR.

When the dichloride species *cis*-**Caz-1** was mixed with **Caz-1$_{F2}$**, rapid and quantitative reaction was observed, with the monofluorinated compound being the only product formed (Table 3, entry 1), which is in marked contrast with the Braddock findings. Furthermore, complete fluorination of *trans*-**Caz-1** can be achieved, requiring a longer reaction time (Table 3, entry 4). This is of great interest considering that the formation of this compound from *trans*-**Caz-1** was found problematic when using the AgF-promoted Cl exchange route (Table 1, entries 4 and 5). In addition, comparison of the rate of isomerization of *trans*-**Caz-1** to *cis*-**Caz-1** with the rate of fluorination of *trans*-**Caz-1** by **Caz-1$_{F2}$** showed that the latter process is faster, which is again in contrast with the results obtained with AgF.[17] These results prompted us to investigate the fluorination of **Ind-II**, **Ind-III**, and **Hov-II** using **Caz-1$_{F2}$**. Unfortunately, no selective formation of fluorinated compounds was observed in these instances.[18]

Computational Studies. Insights into the stability of the Ru complexes isolated in this work and their corresponding trans species were obtained using a computational DFT approach (Table 4).[19] As can be seen in Table 4, the energy values are clearly affected by the relative stability of the free chloride and free fluoride anions in solution.

Focusing on the cis complexes, the replacement of one chloride ligand of *cis*-**Caz-1** by one fluoride ligand, leading to **Caz-1$_F$** + Cl$^-$, is favored by 18.9 kcal/mol (Table 4). In agreement with the experiments, the most stable isomer of **Caz-1$_F$** presents the fluoride ligand trans to the P(O^{i}Pr)$_3$ ligand. The isomer with the fluoride ligand trans to the NHC ligand is 11.6 kcal/mol higher in energy. Substitution of the second chloride atom in the trans isomer, that is, the one with the P(O^{i}Pr)$_3$ ligand trans to the NHC ligand, is less favored than the substitution of

DOI: 10.1021/acscatal.5b00219
ACS Catal. 2015, 5, 3932−3939

Table 4. Energetics (kcal/mol) of the Chloride Exchange Reactions

Caz-1 + 2F$^-$ ⟶ **Caz-1$_F$** + F$^-$ + Cl$^-$ ⟶ **Caz-1$_{F2}$** + 2Cl$^-$

isomer	**Caz-1** + 2F$^-$	**Caz-1$_F$** + F$^-$ + Cl$^-$	**Caz-1$_{F2}$** + 2Cl$^-$
cis	0.0	−18.9	−32.6
trans	+6.8	−7.3	−17.9
trans−cis	+6.8	+11.6	+14.7

the second chloride in the cis isomer (see Table 4); however, it is worth noting that in **Caz-1**, the cis isomer is only 6.8 kcal/mol more stable than the trans isomer, whereas in **Caz-1$_F$** and **Caz-1$_{F2}$**, this preference increases to 11.6 and 14.7 kcal/mol, respectively. Finally, combination of the energy values of the three cis species in Table 4 indicates that the formation of 2 mol of **Caz-1$_F$** by mixing 1 mol of *cis*-**Caz-1** and 1 mol of **Caz-1$_{F2}$** is favored by 5.2 kcal/mol. Overall, these results are consistent with the experimental data showing that when *cis*-**Caz-1** is reacted with 1 equiv of AgF, only **Caz-1$_F$** is formed, and when *cis*-**Caz-1** is reacted with *cis*-**Caz-1$_{F2}$**, only **Caz-1$_F$** is still obtained.

A better understanding of the relative strength of the different Ru−halide bonds in these systems was achieved with bond-snapping-energy calculations (BSE) which is the energy required for the dissociation of the Ru−X bond (see Table 5). In these

Table 5. Ru−X Bond-Snapping Energy in CH_2Cl_2 (kcal/mol)

	precatalyst	atom	heterolytic BSE	homolytic BSE
1	*cis*-**Caz-1**	Cl trans to NHC	31.5	79.0
2	*cis*-**Caz-1**	Cl trans to P	21.7	84.3
3	*cis*-**Caz-1$_F$**	Cl trans to NHC	30.9	85.1
4	*cis*-**Caz-1$_F$**	F trans to P	40.6	110.4
5	*trans*-**Caz-1**	equivalent Cl	36.0	92.8
6	*trans*-**Caz-1$_{F2}$**	equivalent F	47.5	116.1
7	*trans*-**Caz-1$_F$**	F trans to Cl	47.2	114.1
8	*trans*-**Caz-1$_F$**	Cl trans to F	37.4	97.2
9	*cis*-**Caz-1$_{F2}$**	F trans to NHC	43.5	110.2
10	*cis*-**Caz-1$_{F2}$**	F trans to P	40.3	113.7

calculations, the geometry of the [Ru] fragment is kept rigid, and we calculated both homolytic and heterolytic BSEs, which means fragmenting the complex into radical and neutral [Ru]· and X· fragments or into cationic [Ru]$^+$ and anionic X$^-$ fragments, respectively. The BSEs in Table 5 indicate that all the Ru−F BSEs are stronger than the BSE for the corresponding Ru−Cl bond, independently from homo or heterolytic fragmentation of the complexes. This allows us to conclude that the Ru−F bond is stronger than the corresponding Ru−Cl bond. More specifically, the data reported in Table 5 clearly indicate that the Ru−F bonds in *cis*-**Caz-1$_{F2}$** are roughly 12−18 kcal/mol stronger than the corresponding Ru−Cl bonds in *cis*-**Caz-1**. Moreover, for the same complexes, the Ru-halide bond trans to the P(O^{i}Pr)$_3$ ligand is from 3 to 10 kcal/mol weaker than the Ru-halide bond trans to the NHC ligand (comparing entries 9 and 10 as well as entries 1 and 2 in Table 5), suggesting that it is the Ru-halide bond trans to the P atom that undergoes dissociation. Focusing on *cis*-**Caz-1$_F$**, the Ru−Cl bond is weaker than the Ru−F bond (comparing entries 3 and 4 in Table 5), despite the chloride ligand being trans to the NHC ligand. Finally, the strength of the Ru−Cl bond trans to the NHC ligand is nearly the same in *cis*-**Caz-1** and *cis*-**Caz-1$_F$** (comparing entries 1 and 3 in Table 5). Focusing on *trans*-**Caz-1**, in agreement with our previous work,[20] calculations indicate that the Ru−Cl bond is stronger when it is trans to another Cl atom rather than to a P atom (comparing entries 2 and 5 in Table 5).

To gauge if the increased strength of the Ru−F bond relative to the Ru−Cl bond is electrostatic in nature or is due to increased back-donation from the F ligand to the Ru center through a push−pull effect induced by the π-acid phosphite, we performed an energy decomposition analysis (EDA) of the Ru−X bond in *cis*-**Caz-1** and *cis*-**Caz-1$_{F2}$** (see Table 6). We briefly remind the

Table 6. Decomposition Analysis of the Bond-Snapping Energy of Selected Ru−X Bonds in the Gas Phase[a]

	E_{El}	E_{Pauli}	E_{Orb}	BSE
cis-**Caz-1**	−154.7	117.5	−77.9	−115.0
cis-**Caz-1$_{F2}$**	−168.3	122.7	−92.6	−138.1
cis-**Caz-1$_F$**	−168.0	119.2	−94.0	−142.8

[a]The total bond-snapping energy is decomposed as −BSE = E_{El} + E_{Pauli} + E_{Orb}. All values in kcal/mol.

reader that the total BSE can be decomposed into three main terms: −BSE = E_{El} + E_{Pauli} + E_{Orb}. E_{El} accounts for stabilizing electrostatic interaction between the two fragments, E_{Pauli} accounts for repulsion between doubly filled molecular orbitals on the two fragments, and E_{Orb} accounts for stabilizing interaction between filled orbitals on one fragment with empty orbitals on the other fragment. Because the EDA is performed on the intrinsic strength of the Ru−X bond, which does not depend on the environment that can only stabilize the two fragments, the EDA is performed in the gas-phase. Focusing on *cis*-**Caz-1** and *cis*-**Caz-1$_{F2}$**, the data reported in Table 6 indicate that the increased strength of the Ru−F bond in *cis*-**Caz-1$_{F2}$** compared with the Ru−Cl bond in *cis*-**Caz-1** is almost 50%−50% shared between the orbital and the electrostatic terms because both are roughly 14−15 kcal/mol stronger in *cis*-**Caz-1$_{F2}$** compared with *cis*-**Caz-1**. Neither of the two terms is clearly dominant. The repulsive Pauli term is instead rather similar. This suggests that the increased strength of the Ru−F bond is equally a consequence of an increased ionic character of the bond, due to the higher electronegativity of the F atom, and of an increased orbital interaction, which can be probably correlated to back-donation from the F ligand to the Ru center through a push−pull effect. Comparison between *cis*-**Caz-1$_{F2}$** and *cis*-**Caz-1$_F$** indicates that the halide trans to the NHC ligand has a small impact on the Ru−F bond trans to the phosphite.

Catalytic Studies in Ring-Closing Metathesis (RCM). The catalytic activities of both **Caz-1$_{F2}$** and **Caz-1$_F$** were first examined in the RCM of the challenging substrate *N*,*N*-bis(2-methylallyl)tosylamide **1**, and compared with the catalytic activity of the dichloro analogue *cis*-**Caz-1**. Because thermal activation is required to efficiently promote such a reaction, a first comparative study at different temperatures was carried out (Figure 5).[13,21] As can be seen in Figure 5, although the monofluoride performs very well, the difluoride analogue leads to poor conversion to **2** (max. 33% at 110 °C). Comparison of *cis*-**Caz-1** with its monofluoride analogue **Caz-1$_F$** shows that, although the catalytic activity of the dichloride derivative reaches its maximum at 90 °C (79%), the activity of the monofluoride derivative carries on increasing with temperature (84% at 120 °C). This result is even more striking if we compare the catalytic profile of the ring-closing reaction of the three complexes at 110 °C (Figure 6). Under such conditions, *cis*-**Caz-1** has a rapid rate of reaction, followed by a rapid catalyst deactivation (87% conversion within 15 min), whereas **Caz-1$_F$** has an induction

DOI: 10.1021/acscatal.5b00219
ACS Catal. 2015, 5, 3932−3939

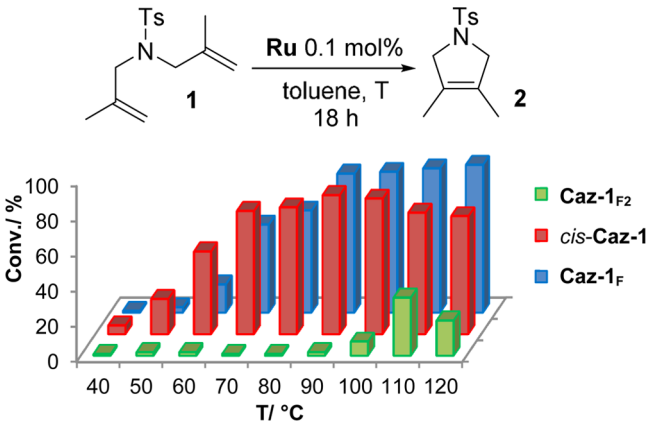

Figure 5. Temperature dependence in the RCM investigated.

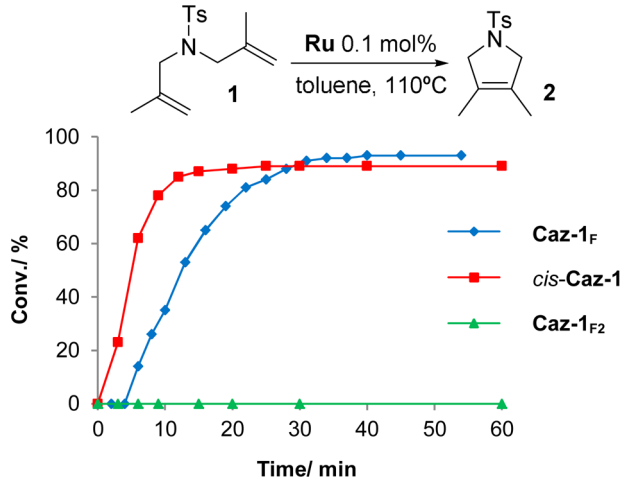

Figure 6. Reaction profiles of *cis*-**Caz-1**, **Caz-1**$_{F}$, and **Caz-1**$_{F2}$ in the RCM of **1** (lines are visual aids and not curve fits).

period of ~3 min and reaches 93% conversion within 40 min. On the other hand, the difluoro species, **Caz-1**$_{F2}$, is poorly active under such reaction conditions (6% conversion after 2 h, and 21% after 24h).[22] It should be noted that *cis*-**Caz-1** outperformed other commercially available precatalysts (such as **Ind-II**, **Hov-II**, and **Ind-III**) in the RCM of substrate **1** under similar conditions,[13a,c] thus suggesting that **Caz-1**$_{F}$ could be a serious contender for this transformation.

To shed light on the formation of the catalytically active species, further DFT calculations were undertaken. For this purpose, we investigated the possible mechanism leading to formation of the classic 14e^{-} intermediate, with the Ru atom presenting a vacant coordination position trans to the NHC ligand for substrate coordination. Starting from the cis isomers, two mechanisms can be envisaged. The first corresponds to concerted cis-to-trans isomerization of the complex with the phosphite still coordinated to the ruthenium, followed by phosphite dissociation. The second corresponds to dissociation of the phosphite from the cis isomer, followed by isomerization of the resulting 14e^{-} intermediate, presenting one halide trans to the NHC ligand, to the most stable 14e^{-} intermediate with a vacant coordination site trans to the NHC ligand.

According to calculations, the barrier for the concerted cis–trans isomerization of the phosphite coordinated species is 35.0, 42.1, and 42.3 kcal/mol for **Caz-1**, **Caz-1**$_{F}$, and **Caz-1**$_{F2}$, respectively, leading to the trans isomers at 6.8, 11.6, and 14.7 kcal/mol above the corresponding cis isomer (see Table 4). To complete this pathway, phosphite dissociation from the trans isomers costs 6.1, 6.0, and 3.9 kcal/mol (*trans*-**Caz-1**, *trans*-**Caz-1**$_{F}$, and *trans*-**Caz-1**$_{F2}$, respectively). As for the stepwise activation mechanism, we were not able to locate a stable geometry for the 14e^{-} intermediate with a halide trans to the NHC ligand. In all cases, this intermediate collapsed to the most stable geometry with the two halides trans to each other. This suggests that phosphite dissociation from the cis isomer triggers, and is concerted with, the rearrangement of the Ru moiety to the most stable 14e^{-} intermediate with the vacancy trans to the NHC ligand. We thus located the transition state for this process, and we found barriers of 28.8, 35.8, and 37.1 for **Caz-1**, **Caz-1**$_{F}$ and **Caz-1**$_{F2}$, respectively. Comparison between the two mechanisms thus indicates that the most likely mechanism for activation of the cis complexes consists in the dissociation of the phosphite with concerted isomerization of the Ru moiety to generate the 14e^{-} intermediate with a vacant coordination position trans to the Ru atom. Furthermore, the trend in the energy of the transition states for phosphite dissociation from the cis complexes, easier for **Caz-1** and more difficult for **Caz-1**$_{F2}$, is consistent with the trend observed for the metathesis activity of Figures 5 and 6. As a remark, we note that we are somewhat overestimating the barrier for phosphite dissociation for **Caz-1**$_{F}$, which should be closer to the barrier calculated for **Caz-1**.

Finally, the beneficial effect of using a fluorinated aromatic solvent was examined for all three complexes (Figure 7). As

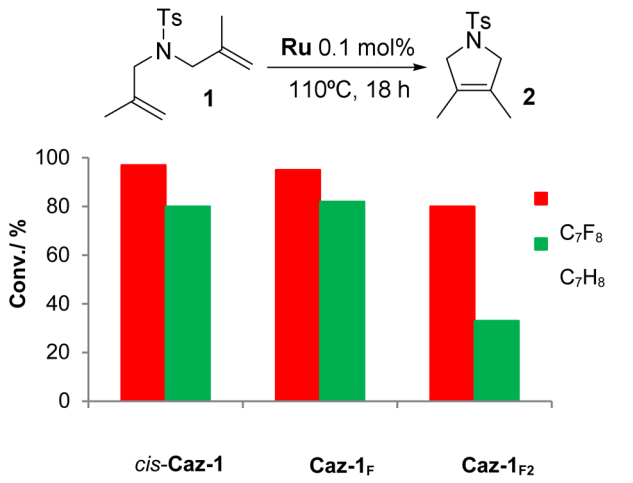

Figure 7. RCM properties of Ru–F precatalysts and *cis*-**Caz-1** in toluene and perfluorotoluene under inert atmosphere.

previously suggested by DFT calculations,[23] an aromatic solvent molecule can stabilize the 14e^{-} species by direct coordination to the Ru center. The same calculations indicated that fluorinated aromatic solvent molecules interact remarkably more strongly than their nonfluorinated counterpart, and this result was correlated to the higher catalytic activity of Ru catalysts in olefin metathesis. This is consistent with the results depicted in Figure 7 because in all cases, catalytic activity is improved when the reaction is carried out in perfluorotoluene.

Scope of the reaction. The catalytic efficiency of the monofluoride complex was next investigated, in a conventional solvent (toluene), at 110 °C (Figure 8). **Caz-1**$_{F}$ proved highly active at 0.1 mol % for hindered and unhindered malonate and tosylate derivatives. With 0.5 mol % loading, **Caz-1**$_{F}$ enables

DOI: 10.1021/acscatal.5b00219
ACS Catal. 2015, 5, 3932–3939

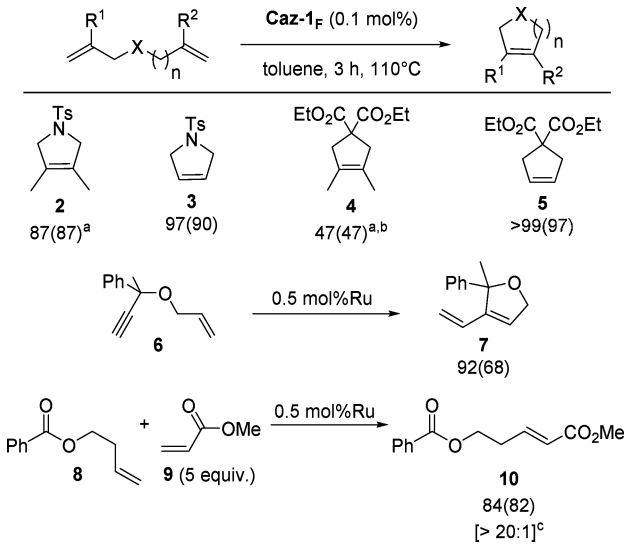

Figure 8. Scope of the reaction employing **Caz-1$_F$**. Reaction conditions: **Caz-1$_F$** (0.1 mol %), substrate (0.25 mmol), toluene (0.5 mL), 3 h, 110 °C, under Ar; average of 2 runs; conversions were determined by GC; isolated yield in parentheses.
[a]Reaction in neat substrate; [b]0.5 mol % Ru, isolated as mixture, NMR yield; [c]*E*/*Z* ratio determined by ^{1}H NMR.

enyne metathesis of **6** as well as the efficient and selective cross-metathesis of **8** with **9**.

CONCLUSION

The synthesis of the first Ru−F precatalysts for olefin metathesis reactions has been presented. *cis*-**Caz-1** reacts with AgF under mild conditions, rather than HF or equivalent reactants, affording isolable Ru−F species. Both **Caz-1$_F$** and **Caz-1$_{F2}$** display the same cis geometry as their chloride precursor. In analogy to what has been observed by Caulton and co-workers with carbonyl complexes, a push−pull interaction involving the fluoride ligand (π-donor) and L-type ligands (π-acceptor) is invoked to stabilize the complexes (F−Ru(II)−P(OR)$_3$ bonding). Fluoride exchange reactions involving **Caz-1$_{F2}$** with *cis*-**Caz-1** and *trans*-**Caz-1** were performed. The selectivity toward only one product (**Caz-1$_F$**) rather than an equilibrium mixture supports the push−pull effect in the F−Ru(II)−P(OR)$_3$ bonding as a driving force for the process. Computational studies confirmed the stability of these complexes when compared with *cis*-**Caz-1**, with **Caz-1$_{F2}$** being the most stable. The stability of the cis precatalysts influences their catalytic activity. A larger energy barrier was observed for **Caz-1$_F$** experimentally and in the computational study compared with *cis*-**Caz-1**. Nevertheless, both precatalysts display similar reactivity in olefin metathesis. **Caz-1$_{F2}$** is less active than the former precatalysts because of its higher stability in the cis form and the very small amount of active species generated. The effect of fluorinated solvents in catalysis was investigated. An overall enhancement of the catalytic activity was observed even for **Caz-1$_{F2}$**, supporting the hypothesis of a stabilization of the NHC-Ru species by the fluorinated solvent rather than the fluorination of active species during the reaction. The catalytic results reported here are not as superior as predicted by the literature reports having computationally addressed *trans*-Ru−F species. In the present work, the cis geometry of the species has an influence on the activity of the complexes, resulting in different catalytic properties compared wtih the hypothetical *trans*-Ru−F species. Although the search for a viable synthetic route leading to this species still remains elusive, the present experimental/computational study clearly highlights that this goal is, indeed, a worthy one. Efforts in this direction and in directions leading to longer living and more active metathesis catalysts are ongoing in our laboratory.

EXPERIMENTAL SECTION

[Ru(Cl)F(Ind)(SIMes){P(O^{i}Pr)$_3$}], Caz-1$_F$. Under an inert atmosphere of argon, AgF (52.2 mg, 0.41 mmol) was added to a solution of *cis*-**Caz-1** (303 mg, 0.34 mmol) in dichloromethane (10 mL).[24] The reaction mixture was stirred for 24 h at room temperature in the absence of light. The solution was filtered, and the solvent was removed in vacuo, leading to the product as a pale-brown solid in a quantitative yield (295 mg, 99%). ^{1}H NMR (CD_2Cl_2, 400 MHz): δ (ppm) = 0.57 (d, $^3J_{HH}$ = 5.9 Hz, 3H, CH−CH_3), 0.75 (d, $^3J_{HH}$ = 6.0 Hz, 3H, CH−CH_3), 0.90 (d, $^3J_{HH}$ = 5.8 Hz, 3H, CH−CH_3), 1.10 (d, $^3J_{HH}$ = 6.0 Hz, 3H, CH−CH_3), 1.38 (d, $^3J_{HH}$ = 6.1 Hz, 3H, CH−CH_3), 1.44 (d, $^3J_{HH}$ = 6.2 Hz, 3H, CH−CH_3), 1.60 (s, 3H, mesityl CH_3), 1.83 (s, 3H, mesityl CH_3), 2.33 (s, 3H, mesityl CH_3), 2.51 (s, 3H, mesityl CH_3), 2.62 (s, 3H, mesityl CH_3), 2.69 (s, 3H, mesityl CH_3), 3.26 (m, 1H, C*H*−CH_3), 3.47−3.58 (m, 1H, carbene H$^{4\prime}$), 3.80−4.03 (m, 3H, carbene H$^{4\prime}$H$^{5\prime}$), 4.26 (m, 1H, C*H*−CH_3), 4.76 (m, 1H, C*H*−CH_3), 6.03 (s, 1H, mesityl CH), 6.32 (s, 1H, indenylidene H^2), 6.51 (s, 1H, mesityl CH), 7.02 (s, 1H, mesityl CH), 7.04 (s, 1H, mesityl CH), 7.15 (d, $^3J_{HH}$ = 7.2 Hz, 1H, indenylidene H^4), 7.29−7.37 (m, 2H, indenylidene H^5 and H^6), 7.37−7.42 (m, 2H, indenylidene H^{10}), 7.43−7.49 (m, 1H, indenylidene H^{11}), 7.67 (d, $^3J_{HH}$ = 7.2 Hz, 2H, indenylidene H^9), 8.93 (d, $^3J_{HH}$ = 7.1 Hz, 1H, indenylidene H^7). ^{13}C−{^{1}H} NMR ($CDCl_3$ 100.6 MHz) δ (ppm) = 17.9 (s, mesityl CH_3), 18.9 (s, mesityl CH_3), 19.1 (s, mesityl CH_3), 20.5 (s, mesityl CH_3), 20.7 (s, mesityl CH_3), 21.2 (s, mesityl CH_3), 24.1 (s, CH−CH_3), 24.2 (s, CH−CH_3), 24.35 (s, CH−CH_3), 24.4 (s, CH−CH_3), 24.5 (s, CH−CH_3), 24.6 (s, CH−CH_3), 51.6 (s, carbene C$^{4\prime}$H), 51.8 (s, carbene C$^{5\prime}$H), 68.8 (d, $^2J_{CP}$ = 11.4 Hz, *C*H−CH_3), 69.9 (d, $^2J_{CP}$ = 9.3 Hz, *C*H−CH_3), 72.6 (bs, *C*H−CH_3), 117.3 (s, indenylidene C^{4}H), 127.5 (s, indenylidene C^{9}H), 128.6 (s, indenylidene C^{11}H), 129.1 (s, indenylidene C^{10}H), 129.4 (s, indenylidene C^{6}H), 129.6 (s, indenylidene C^{5}H), 129.7 (s, mesityl CH), 130.1 (s, mesityl CH), 130.4 (s, mesityl CH), 130.5 (s, indenylidene C^{7}H), 134.5 (s, C^{IV}), 135.3 (s, C^{IV}), 136.3 (s, C^{IV}), 136.8 (s, C^{IV}), 137.0 (s, C^{IV}), 138.1 (bs, 2 C^{IV}), 138.7 (s, C^{IV}), 139.0 (s, C^{IV}), 139.8 (d, $^3J_{CP}$ = 14.6 Hz, indenylidene C^2), 140.2 (s, C^{IV}), 141.6 (m, indenylidene C^{7a}), 142.9 (s, C^{IV}), 209.1 (d, $^2J_{CP}$ = 16.0 Hz, carbene C$^{2\prime}$), 289.6 (d, $^2J_{CP}$ = 25.5 Hz, indenylidene C^1). ^{31}P−{^{1}H} NMR (CD_2Cl_2, 162 MHz) δ (ppm) = 131.4 (d, $^2J_{PF}$ = 286 Hz, P(O^{i}Pr)$_3$). ^{19}F−{^{1}H} NMR (CD_2Cl_2, 282.2 MHz) δ (ppm) = −217.2 (d, $^2J_{PF}$ = 286 Hz, F). Elem. anal. calcd. for $C_{45}H_{57}ClFN_2O_3PRu$: C, 62.81; H, 6.68; N, 3.26. Found: C, 62.72; H, 6.59; N, 3.16.

[RuF$_2$(Ind)(SIMes){P(O^{i}Pr)$_3$}], Caz-1$_{F2}$. Under inert atmosphere, AgF (104 mg, 0.82 mmol) was added to a solution of *cis*-**Caz-1** (298 mg, 0.34 mmol) in dichloromethane (10 mL).[25] The reaction mixture was stirred for 24 h at room temperature in the absence of light. The solution was filtered, and the solvent was removed in vacuo, leading to the product as a pale-brown solid in a quantitative yield (280 mg, 98%). ^{1}H NMR (CD_2Cl_2, 400 MHz): δ (ppm) = 0.5−1.5 (m, 18H, CH−CH_3), 1.66 (s, 3H, mesityl CH_3), 1.83 (s, 3H, mesityl CH_3), 2.37 (s, 3H, mesityl CH_3), 2.40 (s, 3H, mesityl CH_3), 2.65 (s, 3H, mesityl CH_3), 2.68 (s, 3H, mesityl CH_3), 3.46−3.58 (m, 1H, carbene H$^{4\prime}$), 3.80−

DOI: 10.1021/acscatal.5b00219
ACS Catal. 2015, 5, 3932−3939

4.00 (m, 3H, carbene $H^{4'}H^{5'}$), 6.01 (s, 1H, mesityl CH), 6.38 (s, 1H, indenylidene H^2), 6.43 (s, mesityl CH), 7.08 (s, 1H, mesityl CH), 7.09 (s, 1H, mesityl CH), 7.16 (d, $^3J_{HH}$ = 7.1 Hz, 1H, indenylidene H^4), 7.30 (dd, $^3J_{HH}$ = 7.1 Hz, $^3J_{HH}$ = 7.4 Hz, 2H, indenylidene H^5), 7.35 (dd, $^3J_{HH}$ = 7.1 Hz, $^3J_{HH}$ = 7.4 Hz, 2H, indenylidene H^6), 7.40 (dd, $^3J_{HH}$ = 7.5 Hz, $^3J_{HH}$ = 7.5 Hz, 2H, indenylidene H^{10}), 7.47 (dd, $^3J_{HH}$ = 7.2 Hz, $^3J_{HH}$ = 7.4 Hz, 1H indenylidene H^{11}), 7.67 (d, $^3J_{HH}$ = 7.5 Hz, 2H, indenylidene H^9), 9.02 (d, $^3J_{HH}$ = 7.0 Hz, 1H, indenylidene H^7). The isopropyl protons were observed clearly at lower temperature: ^{1}H NMR (CD_2Cl_2, 400 MHz, 223 K): δ (ppm) = 3.16 (m, 1H, C*H*−CH_3), 3.50 (m, 1H, C*H*−CH_3), 4.64 (m, 1H, C*H*−CH_3). ^{13}C−{^{1}H} NMR ($CDCl_3$ 100.6 MHz,) δ (ppm) = 17.5 (s, mesityl CH_3), 18.1 (s, mesityl CH_3), 18.6 (s, mesityl CH_3), 20.4 (s, mesityl CH_3), 20.8 (s, mesityl CH_3), 21.2 (s, mesityl CH_3), 23.6−24.7 (bs, 6 CH−CH_3), 51.4 (s, carbene $C^{4'}H$), 51.8 (s, carbene $C^{5'}H$), 117.0 (s, indenylidene C^4H), 127.3 (s, indenylidene C^9H), 128.3 (s, indenylidene $C^{11}H$), 129.0 (s, indenylidene $C^{10}H$), 129.1 (s, indenylidene C^6H), 129.3 (s, indenylidene C^5H), 129.5 (s, mesityl CH), 130.1 (s, mesityl CH), 130.2 (s, mesityl CH), 130.3 (s, indenylidene C^7H), 135.1 (s, C^{IV}), 135.7 (s, C^{IV}), 136.5 (s, C^{IV}), 136.7 (s, C^{IV}), 137.1 (s, C^{IV}), 137.9 (bs, 2 C^{IV}), 139.0 (s, C^{IV}), 139.1 (s, C^{IV}), 140.2 (d, $^3J_{CP}$ = 14.3 Hz, indenylidene C^2), 140.4 (s, C^{IV}), 141.3 (m, indenylidene C^{7a}), 142.1 (s, C^{IV}). Characteristic peaks were observed at lower temperature (more complicated spectrum due to limited rotation of the ligands): ^{13}C−{^{1}H} NMR ($CDCl_3$ 100.6 MHz, 223 K) δ (ppm) = 68.4 (d, $^2J_{CP}$ = 10.2 Hz, CH−CH_3), 69.4 (d, $^2J_{CP}$ = 7.4 Hz, C*H*−CH_3), 72.0 (bs, $^2J_{CP}$ = 3.6 Hz, C*H*−CH_3), 211.1 (m, carbene $C^{2'}$), 287.0 (m, indenylidene C^1). ^{31}P−{^{1}H} NMR (CD_2Cl_2, 162 MHz) δ (ppm) = 131.5 (d, $^2J_{PF}$ = 286 Hz, $P(O^iPr)_3$). ^{19}F−{^{1}H} NMR (CD_2Cl_2, 376.3 MHz) δ (ppm) = −237.2 (br.s, $F_{transNHC}$), −217.7 (d, $^2J_{PF}$ = 286 Hz, $F_{transPhosphite}$). Elem. anal. calcd for $C_{45}H_{57}F_2N_2O_3PRu$: C, 64.04; H, 6.81; N, 3.32. Found: C, 64.03; H, 6.89; N, 3.39.

■ ASSOCIATED CONTENT

Supporting Information

The Supporting Information is available free of charge on the ACS Publications website at DOI: 10.1021/acscatal.5b00219

Procedures for catalysis, NMR spectra of complexes and catalysis products, procedures and NMR spectra for fluoride exchange reactions and isomerization study (PDF)

Crystallographic data and structure refinement for complexes **Caz-1$_F$** and **Caz-1$_{F2}$**, computational details (CIF); crystallographic data for complexes **Caz-1$_F$** and **Caz-1$_{F2}$** in CIF format can also be obtained free of charge from the Cambridge Crystallographic Data Centre via www.ccdc.cam.ac.uk/data_request/cif (CCDC/911524-911525)

■ AUTHOR INFORMATION

Corresponding Author

*Fax: (+)44 1334 463808. E-mail: cc111@st-andrews.ac.uk.

Notes

The authors declare no competing financial interest.

■ ACKNOWLEDGMENTS

The authors gratefully acknowledge the EC through the seventh framework program (Grant CP-FP 211468-2 EUMET), the Royal Society (University Research Fellowship to C.S.J.C.) for financial support, and Umicore for the gift of *cis*-**Caz-1**.

■ REFERENCES

(1) O'Hagan, D. *Chem. Soc. Rev.* **2008**, *37*, 308−319.

(2) Torrens, H. *Coord. Chem. Rev.* **2005**, *249*, 1957−1985.

(3) (a) Pagenkopf, B. L.; Carreira, E. M. *Tetrahedron Lett.* **1998**, *39*, 9593−9596. (b) Gauthier, D. R.; Carreira, E. M. *Angew. Chem., Int. Ed. Engl.* **1996**, *35*, 2363−2365. (c) Pagenkopf, B. L.; Carreira, E. M. *Chem. - Eur. J.* **1999**, *5*, 3437−3442. (d) Verdaguer, X.; Lange, U. E. W.; Reding, M. T.; Buchwald, S. L. *J. Am. Chem. Soc.* **1996**, *118*, 6784−6785. (e) Dorta, R.; Egli, P.; Zurcher, F.; Togni, A. *J. Am. Chem. Soc.* **1997**, *119*, 10857−10858. (f) Kruger, J.; Carreira, E. M. *J. Am. Chem. Soc.* **1998**, *120*, 837−838. (g) Mezzetti, A.; Becker, C. *Helv. Chim. Acta* **2002**, *85*, 2686−2703. (h) Barthazy, P.; Stoop, R. M.; Wörle, M.; Togni, A.; Mezzetti, A. *Organometallics* **2000**, *19*, 2844−2852.

(4) (a) Pearson, R. G. *J. Am. Chem. Soc.* **1963**, *85*, 3533−3539. (b) Caulton, K. G. *New. J. Chem.* **1994**, *18*, 25−41. (c) Poulton, J. T.; Sigalas, M. P.; Folting, K.; Streib, W. E.; Eisenstein, O.; Caulton, K. G. *Inorg. Chem.* **1994**, *33*, 1476−1485. (d) Doherty, N. M.; Hoffman, N. W. *Chem. Rev.* **1991**, *91*, 553−573. (e) Kiplinger, J. L.; Richmond, T. G.; Osterberg, C. E. *Chem. Rev.* **1994**, *94*, 373−431. (f) Murphy, E. F.; Murugavel, R.; Roesky, H. W. *Chem. Rev.* **1997**, *97*, 3425−3468. (g) Coalter, J. N.; Huffman, J. C.; Streib, W. E.; Caulton, K. G. *Inorg. Chem.* **2000**, *39*, 3757−3764. (h) Burch, R. R.; Harlow, R. L.; Ittel, S. D. *Organometallics* **1987**, *6*, 982−987.

(5) (a) Braun, T.; Steffen, A.; Schorlemer, V.; Neumann, B.; Stammler, H. G. *Dalton Trans.* **2005**, 3331−3336. (b) Yahav, A.; Goldberg, I.; Vigalok, A. *Inorg. Chem.* **2005**, *44*, 1547−1553. (c) Cooper, A. C.; Folting, K.; Huffman, J. C.; Caulton, K. G. *Organometallics* **1997**, *16*, 505−507. (d) Brewer, S. A.; Holloway, J. H.; Hope, E. G. *J. Chem. Soc., Dalton Trans.* **1994**, 1067−1071. (e) Brewer, S. A.; Coleman, K. S.; Fawcett, J.; Holloway, J. H.; Hope, E. G.; Russell, D. R.; Watson, P. G. *J. Chem. Soc., Dalton Trans.* **1995**, 1073−1077. (f) Coleman, K. S.; Fawcett, J.; Holloway, J. H.; Hope, E. G.; Russell, D. R. *J. Chem. Soc., Dalton Trans.* **1997**, 3557−3562. (g) Coleman, K. S.; Fawcett, J.; Harding, D. A. J.; Hope, E. G.; Singh, K.; Solan, G. A. *Eur. J. Inorg. Chem.* **2010**, *2010*, 4130−4138. (h) Fawcett, J.; Harding, D. A. J.; Hope, E. G.; Singh, K.; Solan, G. A. *Dalton Trans.* **2009**, 6861−6870. (i) Coleman, K. S.; Holloway, J. H.; Hope, E. G. *J. Chem. Soc., Dalton Trans.* **1997**, 1713−1718. (j) Marshall, C. J.; Peacock, R. D.; Russell, D. R.; Wilson, I. L. *J. Chem. Soc. D* **1970**, 1643−1644. (k) Hewitt, A. J.; Holloway, J. H.; Peacock, R. D.; Raynor, J. B.; Wilson, I. L. *J. Chem. Soc., Dalton Trans.* **1976**, 579−583.

(6) Fraser, S. L.; Antipin, M. Y.; Khroustalyov, V. N.; Grushin, V. V. *J. Am. Chem. Soc.* **1997**, *119*, 4769−4770.

(7) Amii, H.; Uneyama, K. *Chem. Rev.* **2009**, *109*, 2119−2183.

(8) (a) Reade, S. P.; Nama, D.; Mahon, M. F.; Pregosin, P. S.; Whittlesey, M. K. *Organometallics* **2007**, *26*, 3484−3491. (b) Reade, S. P.; Mahon, M. F.; Whittlesey, M. K. *J. Am. Chem. Soc.* **2009**, *131*, 1847−1861.

(9) Sanford, M. S.; Love, J. A.; Grubbs, R. H. *J. Am. Chem. Soc.* **2001**, *123*, 6543−6554.

(10) Naumov, S.; Buchmeiser, M. R. *J. Phys. Org. Chem.* **2008**, *21*, 963−970.

(11) (a) Seiders, T. J.; Ward, D. W.; Grubbs, R. H. *Org. Lett.* **2001**, *3*, 3225−3228. (b) Krause, J. O.; Nuyken, O.; Wurst, K.; Buchmeiser, M. R. *Chem. - Eur. J.* **2004**, *10*, 777−784. (c) Halbach, T. S.; Mix, S.; Fischer, D.; Maechling, S.; Krause, J. O.; Sievers, C.; Blechert, S.; Nuyken, O.; Buchmeiser, M. R. *J. Org. Chem.* **2005**, *70*, 4687−4694. (d) Tanaka, K.; Böhm, V. P. W.; Chadwick, D.; Roeper, M.; Braddock, D. C. *Organometallics* **2006**, *25*, 5696−5698.

(12) (a) Gawin, R.; Grela, K. *Eur. J. Inorg. Chem.* **2012**, *2012*, 1477−1484. (b) Caskey, S. R.; Stewart, M. H.; Ahn, Y. J.; Johnson, M. J. A.; Rowsell, J. L. C.; Kampf, J. W. *Organometallics* **2007**, *26*, 1912−1923.

(13) (a) Bantreil, X.; Schmid, T. E.; Randall, R. A. M.; Slawin, A. M. Z.; Cazin, C. S. J. *Chem. Commun.* **2010**, *46*, 7115−7117. (b) Schmid, T. E.; Bantreil, X.; Citadelle, C. A.; Slawin, A. M. Z.; Cazin, C. S. J. *Chem. Commun.* **2011**, *47*, 7060−7062. (c) Songis, O.; Slawin, A. M. Z.; Cazin,

DOI: 10.1021/acscatal.5b00219
ACS Catal. 2015, 5, 3932−3939

C. S. J. *Chem. Commun.* **2012**, *48*, 1266−1268. (d) Bantreil, X.; Poater, A.; Urbina-Blanco, C. A.; Bidal, Y. D.; Falivene, L.; Randall, R. A. M.; Cavallo, L.; Slawin, A. M. Z.; Cazin, C. S. J. *Organometallics* **2012**, *31*, 7415−7426. (e) Urbina-Blanco, C. A.; Bantreil, X.; Wappel, J.; Schmid, T. E.; Slawin, A. M. Z.; Slugovc, C.; Cazin, C. S. J. *Organometallics* **2013**, *32*, 6240−6247. (f) Leitgeb, A.; Wappel, J.; Urbina-Blanco, C. A.; Strasser, S.; Wappl, C.; Cazin, C. S. J.; Slugovc, C. *Monatsh. Chem.* **2014**, *145*, 1513−1517.

(14) See Supporting Information, section 3 page S10.

(15) CCDC-911524 contains the supporting crystallographic data for **Caz-1**$_{F}$. These data can be obtained free of charge from the Cambridge Crystallographic Data Centre via www.ccdc.cam.ac.uk/data_request/cif.

(16) CCDC-911525 contains the supporting crystallographic data for **Caz-1**$_{F2}$. These data can be obtained free of charge from the Cambridge Crystallographic Data Centre via www.ccdc.cam.ac.uk/data_request/cif.

(17) See Supporting Information section 5, page S12.

(18) See Supporting Information section 5.2, page S13.

(19) See computational details in the Supporting Information.

(20) Falivene, L.; Poater, A.; Cazin, C. S. J.; Slugovc, C.; Cavallo, L. *Dalton Trans.* **2013**, *42*, 7312−7317.

(21) Slugovc, C.; Perner, B.; Stelzer, F.; Mereiter, K. *Organometallics* **2004**, *23*, 3622−3626.

(22) See Supporting Information section 6.3, page S16.

(23) Samojłowicz, C.; Bieniek, M.; Pazio, A.; Makal, A.; Wozniak, K.; Poater, A.; Cavallo, L.; Wojcik, J.; Zdanowski, K.; Grela, K. *Chem. - Eur. J.* **2011**, *17*, 12981−12993.

(24) The granulometry of AgF has an impact on the efficiency of the chloride exchange reaction in such heterogeneous conditions; see ref 6.

DOI: 10.1021/acscatal.5b00219
ACS Catal. 2015, 5, 3932−3939